Sequential Learning of SAR Image Time Series for Earth Deformation Monitoring

Doctoral Thesis Defense

Dana El Hajjar

9 december 2025

Supervised by	Yajing Yan	University Savoie Mont Blanc
Co-supervised by	Mohammed Nabil El Korso Guillaume Ginolhac	University Paris-Saclay University Savoie Mont Blanc

Laboratoire Signaux & Systèmes

LISTIC

agence nationale de la recherche

Content

Content

SAR image

Single Look Complex (SLC) is characterized by a **complex** signal

$$\boxed{z = a \cdot e^{j\theta}}$$

- **Amplitude (a)**: strength of the backscattering
- **Phase (θ)**: geometric information, random information $\theta = \theta_{\text{random}} + \theta_{\text{geometric}}$

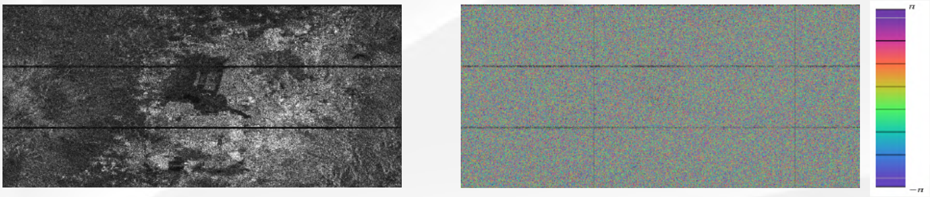

(a) amplitude (b) phase

Figure: Sentinel-1 SAR image over Mexico City

Interferogram

2 coregistered SLC images of the same scene at different times → **interferogram**

$$I = \frac{\sum_{i,j\in\Omega} z_1(i,j) z_2^*(i,j)}{\sqrt{\sum_{i,j\in\Omega} z_1(i,j) z_1^*(i,j) \sum_{i,j\in\Omega} z_2(i,j) z_2^*(i,j)}} = \gamma e^{j\Delta\theta}$$

where

- Ω is the spatial neighborhood of the pixel (i,j)
- γ is **coherence** ($\in [0,1]$), representing the similarity between the two images
- $\Delta\theta$ represents the **phase difference** ($\Delta\theta = \theta_1 - \theta_2$, $\theta \in [-\pi, \pi]$)

(a) coherence

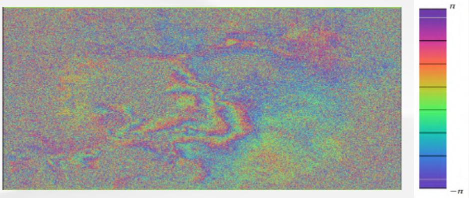

(b) phase difference

Figure: Interferogram over Mexico City

Interferometric phase

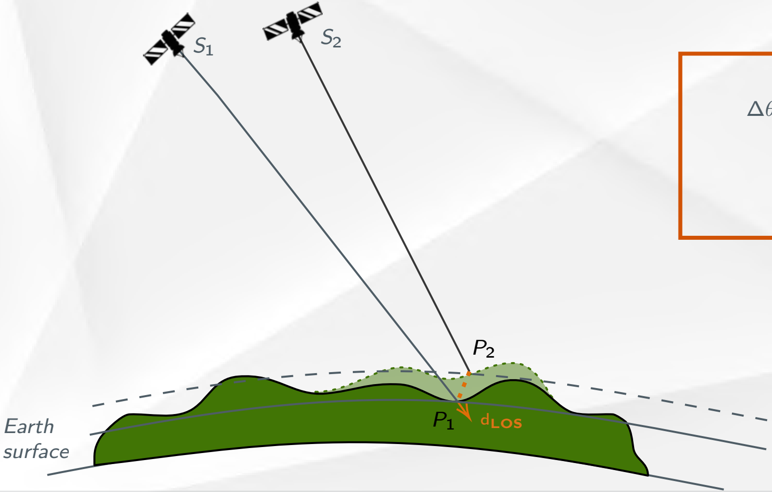

$$\Delta\theta = \Delta\theta_{orb} + \Delta\theta_{topo} + \Delta\theta_{atm} + \boldsymbol{\Delta\theta_{def}} + \Delta\theta_{noise}$$

$$\frac{4\pi}{\lambda} \boldsymbol{d_{LOS}}$$

Multi-temporal InSAR

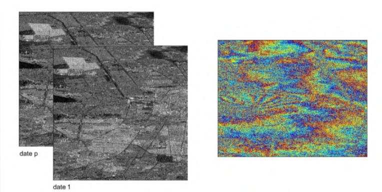

Interferogram of 2 SLC images

- Decorrelation noise
- Atmospheric disturbances
- Measurement accuracy (centimetric)

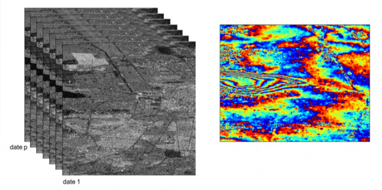

Multi-temporal interferograms

- Building **interferometric networks** from a **time series** of SAR images
- **Continuous** monitoring of Earth deformations
- Improvement in measurement accuracy (millimetric)

Content

Data model: covariance matrix structure

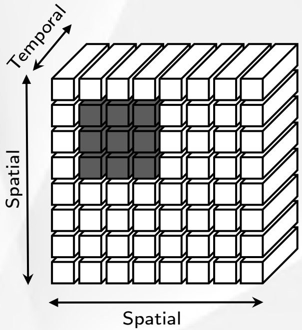

Figure: Representation of SAR time series using a sliding window of size n pixels [6]

Consider a multivariate random vector $\mathbf{x} = [x_1, \ldots, x_p]^T$
For all $(l, k) \in \{1, \ldots, p\}^2$,

$$x_l = a_l e^{j\theta_l}, \qquad x_k = a_k e^{j\theta_k}$$

The second-order moment

$$\mathbb{E}[x_l (x_k)^*] = \gamma_{k,l} \sigma_k \sigma_l \exp(j(\theta_l - \theta_k))$$

$\longrightarrow$ covariance matrix

$$\boxed{\mathbb{E}[\boldsymbol{x}\boldsymbol{x}^H] \triangleq \boldsymbol{\Sigma} = \boldsymbol{\Psi} \circ (\boldsymbol{w}_\theta \boldsymbol{w}_\theta^H)}$$

where

- $\gamma_{k,l}$: coherence coefficient between x_k and x_l
- σ_l: standard deviation of x_l
- $\boldsymbol{\Sigma}$: covariance matrix
- $\boldsymbol{\Psi}$: coherence matrix
- $\boldsymbol{w}_\theta$: vector of phase exponential

[6] P.V.H. Vu et al. (2023) "Robust Phase Linking in InSAR".

Data model: Gaussian distribution

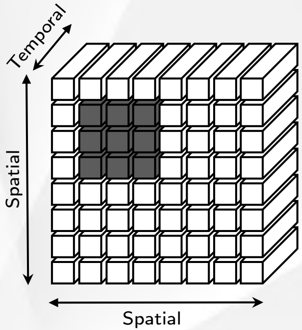

Figure: Representation of SAR time series using a sliding window of size n pixels [6]

Consider a multivariate random vector

$$\boldsymbol{x} = [x_1, \ldots, x_p]^T$$

$\{\boldsymbol{x}^i\}_{i=1}^n \ \forall i \in [1, n]$, a set i.i.d $\longrightarrow \boldsymbol{x} \sim \mathcal{CN}(0, \boldsymbol{\Sigma})$

The log-likelihood is

$$\mathcal{L}(\boldsymbol{x}; \boldsymbol{\Sigma}) = -\log\left(\prod_{i=1}^n f(\boldsymbol{x}^i, \boldsymbol{\Sigma})\right) \propto n\log(|\boldsymbol{\Sigma}|) + n\,\mathrm{Tr}(\boldsymbol{\Sigma}^{-1}\boldsymbol{S})$$

where $\boldsymbol{S} = \frac{1}{n}\sum_{i=1}^n \boldsymbol{x}^i\boldsymbol{x}^{iH}$

Covariance matrix: $\mathbb{E}[\boldsymbol{x}\boldsymbol{x}^H] \triangleq \boldsymbol{\Sigma} = \boldsymbol{\Psi} \circ (\boldsymbol{w}_\theta \boldsymbol{w}_\theta^H)$

[6] P.V.H. Vu et al. (2023) "Robust Phase Linking in InSAR".

Standard Phase Linking (PL)

Principle:
Estimate $p-1$ phase differences from p SAR images $\longrightarrow$ $\boldsymbol{w}_\theta$

[1] A. Guarnieri et al. (2008) "On the exploitation of target statistics for SAR interferometry applications".
[8] P.V.H. Vu et al. (2022) "A new phase linking algorithm for multi-temporal InSAR based on the Maximum Likelihood Estimator".

Standard Phase Linking (PL)

Principle:
Estimate $p-1$ phase differences from p SAR images $\longrightarrow \boldsymbol{w}_{\boldsymbol{\theta}}$

Assuming that $\boldsymbol{\Psi}$ is known, the method is equivalent to optimizing the following problem [1]:

$$\begin{aligned} \underset{\boldsymbol{w}_{\boldsymbol{\theta}}}{\text{minimize}} \quad & \boldsymbol{w}_{\boldsymbol{\theta}}^H(\boldsymbol{\Psi}^{-1} \circ \boldsymbol{S})\boldsymbol{w}_{\boldsymbol{\theta}} \\ \text{subject to} \quad & \theta_1 = 0 \end{aligned}$$

[1] A. Guarnieri et al. (2008) "On the exploitation of target statistics for SAR interferometry applications".
[8] P.V.H. Vu et al. (2022) "A new phase linking algorithm for multi-temporal InSAR based on the Maximum Likelihood Estimator".

Standard Phase Linking (PL)

Principle:
Estimate $p-1$ phase differences from p SAR images $\longrightarrow \boldsymbol{w}_\theta$

Assuming that $\boldsymbol{\Psi}$ is known, the method is equivalent to optimizing the following problem [1]:

$$\begin{aligned} \underset{\boldsymbol{w}_\theta}{\text{minimize}} \quad & \boldsymbol{w}_\theta^H(\boldsymbol{\Psi}^{-1} \circ \boldsymbol{S})\boldsymbol{w}_\theta \\ \text{subject to} \quad & \theta_1 = 0 \end{aligned}$$

PROBLEM !!!
In reality, $\boldsymbol{\Psi}$ is unknown

- [1] proposed to use a plug-in: $\boldsymbol{\Psi}_{mod} = |\boldsymbol{S}| \longrightarrow$ **not optimal**
- [8] proposed to estimate $\boldsymbol{\Psi}$ jointly with $\boldsymbol{w}_\theta$

[1] A. Guarnieri et al. (2008) "On the exploitation of target statistics for SAR interferometry applications".
[8] P.V.H. Vu et al. (2022) "A new phase linking algorithm for multi-temporal InSAR based on the Maximum Likelihood Estimator".

Phase Linking based on Maximum Likelihood Estimation (MLE-PL)

→ The optimization problem [8]

$$
\begin{aligned}
\underset{\boldsymbol{\Psi}, \boldsymbol{w}_{\boldsymbol{\theta}}}{\text{minimize}} \quad & \mathcal{L}(\boldsymbol{x}^i; \boldsymbol{\Sigma}(\boldsymbol{\Psi}, \boldsymbol{w}_{\boldsymbol{\theta}})) \\
\text{subject to} \quad & \theta_1 = 0 \\
& \boldsymbol{w}_{\boldsymbol{\theta}} \in \mathbb{T}_p \\
& \boldsymbol{\Psi} \in \mathbb{S}^p
\end{aligned}
$$

with $\mathbb{T}_p = \{\boldsymbol{w}_{\boldsymbol{\theta}} \in \mathbb{C}^p || [\boldsymbol{w}_{\boldsymbol{\theta}}]_i| = 1, \forall i \in [1, p]\}$ and $\mathbb{S}^p = \{\boldsymbol{A} \in \mathbb{R}^{p \times p} | \boldsymbol{A} = \boldsymbol{A}^T\}$

2 unknowns to estimate $\longrightarrow$ **Block Coordinate Descent Algorithm (BCD)** + **Majorization-Minimization (MM)**

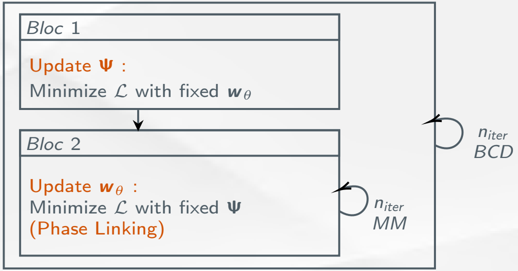

[8] P.V.H. Vu et al. (2022) "A new phase linking algorithm for multi-temporal InSAR based on the Maximum Likelihood Estimator".

Towards a Robust Model: Scaled Gaussian distribution

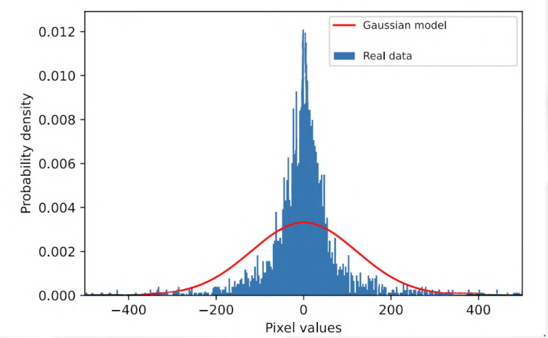

Figure: Empirical distribution of the real part of Sentinel-1 SLC samples taken from a 50 × 50 window on the image acquired on July 3, 2019 [6]

Consider that the set $\{\boldsymbol{x}^i\}_{i=1}^n$ is i.i.d and follows a **Scaled Gaussian** distribution $\boldsymbol{x}^i \sim \mathcal{CN}(0, \tau_i \boldsymbol{\Sigma})$

$$f(\boldsymbol{x}^i) = \frac{1}{\pi^n \det(\tau_i \boldsymbol{\Sigma})} \exp\left(-\boldsymbol{x}^{iH} (\tau_i \boldsymbol{\Sigma})^{-1} \boldsymbol{x}^i\right)$$

The log-likelihood is

$$\mathcal{L}(\boldsymbol{x}; \boldsymbol{\Sigma}, \{\tau_i\}_{i=1}^n) = n \log |\boldsymbol{\Sigma}| + n \mathrm{Tr}\{\boldsymbol{\Sigma}^{-1} \mathrm{S}\} + \sum_{i=1}^{n} p \log \tau_i + \text{const}$$

[6] P.V.H. Vu et al. (2023) "Robust Phase Linking in InSAR".

Robust Phase Linking (MLE-PL)

→ The optimization problem [6]

$$\begin{array}{ll} \underset{\boldsymbol{\Psi}, \boldsymbol{w_\theta}, \{\tau_i\}_{i=1}^n}{\text{minimize}} & \mathcal{L}(\boldsymbol{x}^i; \boldsymbol{\Sigma}(\boldsymbol{\Psi}, \boldsymbol{w_\theta})) \\ \text{subject to} & \theta_1 = 0 \\ & \boldsymbol{w_\theta} \in \mathbb{T}_p \\ & \boldsymbol{\Psi} \in \mathbb{S}^p \end{array}$$

with $\mathbb{T}_p = \{\boldsymbol{w_\theta} \in \mathbb{C}^p | |[\widetilde{\boldsymbol{w}}_{\boldsymbol{\theta}}]_i| = 1, \forall i \in [1, p]\}$ and $\mathbb{S}^p = \{\boldsymbol{A} \in \mathbb{R}^{p \times p} | \boldsymbol{A} = \boldsymbol{A}^T\}$

3 unknowns to estimate $\longrightarrow$ **Block Coordinate Descent Algorithm (BCD)** + **Majorization-Minimization (MM)**

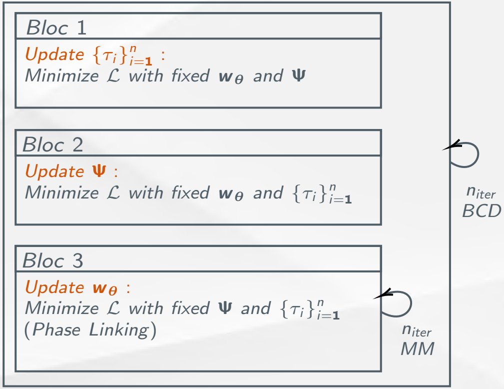

[6] P.V.H. Vu et al. (2023) "Robust Phase Linking in InSAR".

Covariance Fitting Interferometric Phase Linking (COFI-PL)

MLE-PL [6]

$$\begin{aligned} \underset{\boldsymbol{\Psi}, \boldsymbol{w}_{\boldsymbol{\theta}}, \{\tau_i\}_{i=1}^{n}}{\text{minimize}} \quad & \mathcal{L}(\boldsymbol{x}^i; \boldsymbol{\Sigma}(\boldsymbol{\Psi}, \boldsymbol{w}_{\boldsymbol{\theta}})) \\ \text{subject to} \quad & \theta_1 = 0 \\ & \boldsymbol{w}_{\boldsymbol{\theta}} \in \mathbb{T}_p \\ & \boldsymbol{\Psi} \in \mathbb{S}^p \end{aligned}$$

Motivations to COFI-PL:

- phase ambiguity
- reduction of computational cost

[6] P.V.H. Vu et al. (2023) "Robust Phase Linking in InSAR".
[7] P.V.H. Vu et al. (2024) "Covariance Fitting Interferometric Phase Linking: Modular Framework and Optimization Algorithms".

Covariance Fitting Interferometric Phase Linking (COFI-PL)

MLE-PL [6]

$$\begin{array}{ll} \underset{\boldsymbol{\Psi}, \boldsymbol{w}_{\boldsymbol{\theta}}, \{\tau_i\}_{i=1}^n}{\text{minimize}} & \mathcal{L}(\boldsymbol{x}^i; \boldsymbol{\Sigma}(\boldsymbol{\Psi}, \boldsymbol{w}_{\boldsymbol{\theta}})) \\ \text{subject to} & \theta_1 = 0 \\ & \boldsymbol{w}_{\boldsymbol{\theta}} \in \mathbb{T}_p \\ & \boldsymbol{\Psi} \in \mathbb{S}^p \end{array}$$

Motivations to COFI-PL:

- phase ambiguity
- reduction of computational cost

COFI-PL involves refining the structure of the covariance matrix estimator by minimizing a projection criterion [7].

$$\begin{array}{ll} \underset{\boldsymbol{w}_{\boldsymbol{\theta}}}{\text{minimize}} & f_{\boldsymbol{\Sigma}}^d(\boldsymbol{\Sigma}, \boldsymbol{\Psi} \circ \boldsymbol{w}_{\boldsymbol{\theta}} \boldsymbol{w}_{\boldsymbol{\theta}}^H) \\ \text{subject to} & \theta_1 = 0 \\ & \boldsymbol{w}_{\boldsymbol{\theta}} \in \mathbb{T}_p \end{array}$$

[6] P.V.H. Vu et al. (2023) "Robust Phase Linking in InSAR".
[7] P.V.H. Vu et al. (2024) "Covariance Fitting Interferometric Phase Linking: Modular Framework and Optimization Algorithms".

Content

One or several images are on the way . . .

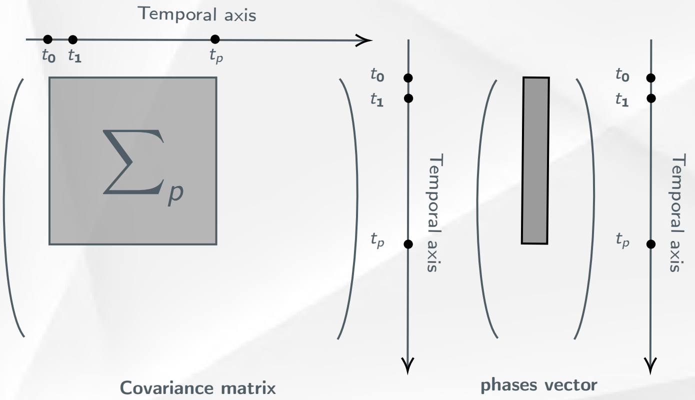

$\forall i = 1, \ldots, n$

$$\tilde{x}^i = \begin{pmatrix} x_1^i \\ x_2^i \\ \vdots \\ x_p^i \end{pmatrix}_{(p)}$$

One or several images are on the way . . .

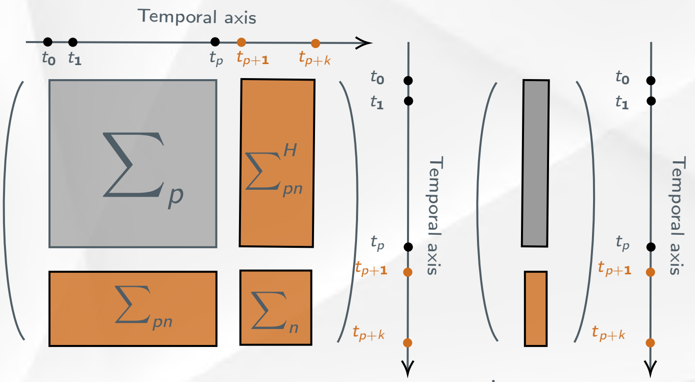

Covariance matrix **phases vector**

$\forall i = 1, \dots, n$

$$\tilde{x}^i = \begin{pmatrix} x^i_1 \\ x^i_2 \\ \vdots \\ x^i_p \end{pmatrix}_{(p)} \rightarrow \tilde{x}^i = \begin{pmatrix} x^i_1 \\ x^i_2 \\ \vdots \\ x^i_p \\ x^i_{p+1} \\ \vdots \\ x^i_{p+k} \end{pmatrix}_{(p+1)}$$

At **each new** SAR acquisition

- **Re-Estimation** of the increasing covariance matrix
- **Re-Estimation** of the phases

$\longrightarrow$ **Huge computation time**

Sequential Estimator (SE)

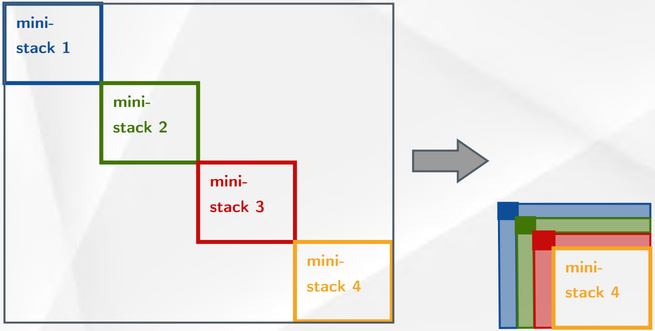

Mini-stack Division: Split the time series into small temporal blocks.

Phase Linking: Estimate relative phases in each mini-stack.

Data compression: Reduce data to one virtual image per block.

Datum connection: Link all mini-stacks and correct phase bias by a PL on all compressed versions.

[4] H. Ansari et al. (2017) "Sequential Estimator: Toward efficient InSAR time series analysis".

Sequential Estimator (SE)

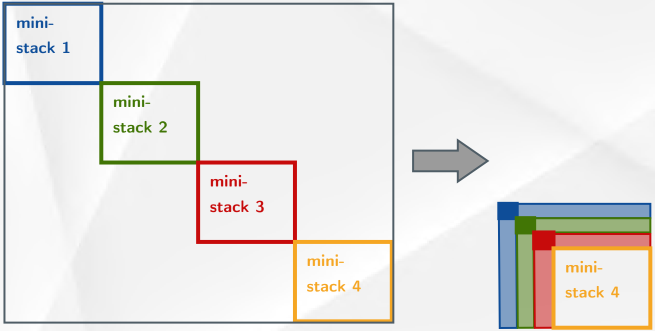

Mini-stack Division: Split the time series into small temporal blocks.

Phase Linking: Estimate relative phases in each mini-stack.

Data compression: Reduce data to one virtual image per block.

Datum connection: Link all mini-stacks and correct phase bias by a PL on all compressed versions.

significant time to assemble meaningful mini-stacks

lack of robustness against various forms of temporal decorrelation

based on Gaussian assumptions for SAR imagery

[4] H. Ansari et al. (2017) "Sequential Estimator: Toward efficient InSAR time series analysis".

Research questions

RECAP

	robustness	sequential
MLE-PL [6]	✓	✗
COFI-PL [7]	✓	✗
SE [4]	✗	✓

[6] P.V.H. Vu et al. (2023) "Robust Phase Linking in InSAR".
[7] P.V.H. Vu et al. (2024) "Covariance Fitting Interferometric Phase Linking: Modular Framework and Optimization Algorithms".
[4] H. Ansari et al. (2017) "Sequential Estimator: Toward efficient InSAR time series analysis".

Research questions

RECAP

	robustness	sequential
MLE-PL [6]	✓	✗
COFI-PL [7]	✓	✗
SE [4]	✗	✓

How can we develop a **sequential** method that is more **cost-effective** than traditional offline approaches while ensuring:

- The **statistical relationship** between historical images and new images remains optimal.
- The integration and **regularization tools** for incorporating new image blocks are maintained.
- The **cost of storage** is minimized.

[6] P.V.H. Vu et al. (2023) "Robust Phase Linking in InSAR".
[7] P.V.H. Vu et al. (2024) "Covariance Fitting Interferometric Phase Linking: Modular Framework and Optimization Algorithms".
[4] H. Ansari et al. (2017) "Sequential Estimator: Toward efficient InSAR time series analysis".

Content

Content

Data model S-MLE-PL

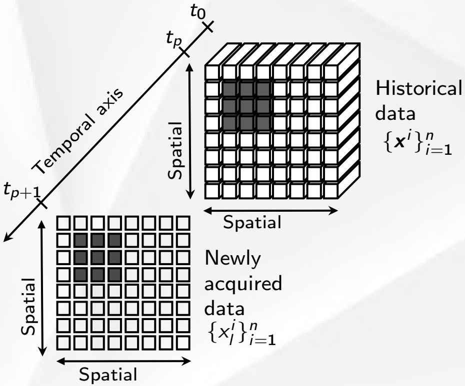

Figure: Representation of SAR time series with a sliding window containing n pixels $\widetilde{\boldsymbol{x}}^i$.

We consider a set $\{\widetilde{\boldsymbol{x}}^i\}_{i=1}^n$ where

$$\widetilde{\boldsymbol{x}}^i = [\underbrace{x_1^i, \ldots, x_p^i}_{\boldsymbol{x}^i}, x_l^i]^T \in \mathbb{C}^{l=p+1}$$

The set $\left\{\widetilde{\boldsymbol{x}}^i\right\}_{i=1}^n$, $\forall i \in [1, n]$, is i.i.d., such that

$$\widetilde{\boldsymbol{x}}^i \sim \mathcal{CN}(0, \tau_i \widetilde{\boldsymbol{\Sigma}}).$$

The covariance matrix can be rewritten as

$$\widetilde{\boldsymbol{\Sigma}} = \begin{pmatrix} \boldsymbol{\Sigma} & w^*_{\theta_l} \operatorname{diag}(\boldsymbol{w_\theta}) \boldsymbol{\gamma}^T \\ \boldsymbol{\gamma} \operatorname{diag}(\boldsymbol{w_\theta})^H w_{\theta_l} & \gamma_l \end{pmatrix}$$

MLE problem

MLE-PL (offline)

$$\underset{\widetilde{\boldsymbol{\Psi}}, \widetilde{\boldsymbol{w}}_{\boldsymbol{\theta}}, \{\tau_i\}_{i=1}^{n}}{\text{minimize}} \quad \mathcal{L}(\widetilde{\boldsymbol{x}}^i; \widetilde{\boldsymbol{\Psi}}, \widetilde{\boldsymbol{w}}_{\boldsymbol{\theta}}, \{\tau_i\}_{i=1}^{n})$$
$$\text{subject to} \quad \theta_{\mathbf{1}} = 0, \widetilde{\boldsymbol{w}}_{\boldsymbol{\theta}} \in \mathbb{T}_l, \widetilde{\boldsymbol{\Psi}} \in \mathbb{S}^l$$

S-MLE-PL (sequential)

$$\underset{\gamma, \gamma_l, w_{\theta_l}, \{\tau_i\}_{i=1}^{n}}{\text{minimize}} \quad \mathcal{L}(\widetilde{\boldsymbol{x}}^i; \boldsymbol{\gamma}, \gamma_l, w_{\theta_l}, \{\tau_i\}_{i=1}^{n})$$
$$\text{subject to} \quad \theta_{\mathbf{1}} = 0, |w_{\theta_l}| = 1, \boldsymbol{\gamma}, \gamma_l \text{ real}$$

[2] T.W. Anderson (1962) "An introduction to multivariate statistical analysis".

MLE problem

MLE-PL (offline)

$$\underset{\widetilde{\boldsymbol{\Psi}}, \widetilde{\boldsymbol{w}}_{\boldsymbol{\theta}}, \{\tau_i\}_{i=1}^n}{\text{minimize}} \quad \mathcal{L}(\widetilde{\boldsymbol{x}}^i; \widetilde{\boldsymbol{\Psi}}, \widetilde{\boldsymbol{w}}_{\boldsymbol{\theta}}, \{\tau_i\}_{i=1}^n)$$
$$\text{subject to} \quad \theta_1 = 0, \widetilde{\boldsymbol{w}}_{\boldsymbol{\theta}} \in \mathbb{T}_l, \widetilde{\boldsymbol{\Psi}} \in \mathbb{S}^l$$

S-MLE-PL (sequential)

$$\underset{\boldsymbol{\gamma}, \gamma_l, w_{\theta_l}, \{\tau_i\}_{i=1}^n}{\text{minimize}} \quad \mathcal{L}(\widetilde{\boldsymbol{x}}^i; \boldsymbol{\gamma}, \gamma_l, w_{\theta_l}, \{\tau_i\}_{i=1}^n)$$
$$\text{subject to} \quad \theta_1 = 0, |w_{\theta_l}| = 1, \boldsymbol{\gamma}, \gamma_l \text{ real}$$

$$\mathcal{L}(\widetilde{\boldsymbol{x}}^i; \boldsymbol{\gamma}, \gamma_l, w_{\theta_l}, \{\tau_i\}_{i=1}^n) = -\sum_{i=1}^{n} \mathcal{L}^i(x_l^i | \boldsymbol{x}^i; \boldsymbol{\gamma}, \gamma_l, w_{\theta_l}, \{\tau_i\}_{i=1}^n) + \mathcal{L}^i(\boldsymbol{x}^i; \{\tau_i\}_{i=1}^n)$$

According to [2], $x_l^i | \boldsymbol{x}^i \sim \mathcal{CN}(\mu_x^i, \sigma_x^2)$ where

- $\mu_x^i = w_{\theta_l} \boldsymbol{\gamma} \text{diag}(\hat{\boldsymbol{w}}_{\boldsymbol{\theta}})^H \hat{\Sigma}^{-1} \boldsymbol{x}^i$
- $\sigma_x^2 = \gamma_l - \boldsymbol{\gamma} \text{diag}(\hat{\boldsymbol{w}}_{\boldsymbol{\theta}})^H \hat{\Sigma}^{-1} \text{diag}(\hat{\boldsymbol{w}}_{\boldsymbol{\theta}}^H) \boldsymbol{\gamma}^T$

[2] T.W. Anderson (1962) "An introduction to multivariate statistical analysis".

MLE problem

MLE-PL (offline)

$$\begin{aligned} &\underset{\widetilde{\boldsymbol{\Psi}},\widetilde{\boldsymbol{w}}_{\boldsymbol{\theta}},\{\tau_i\}_{i=1}^{n}}{\text{minimize}} && \mathcal{L}(\widetilde{\boldsymbol{x}}^i;\widetilde{\boldsymbol{\Psi}},\widetilde{\boldsymbol{w}}_{\boldsymbol{\theta}},\{\tau_i\}_{i=1}^{n}) \\ &\text{subject to} && \theta_1=0,\ \widetilde{\boldsymbol{w}}_{\boldsymbol{\theta}}\in\mathbb{T}_l,\ \widetilde{\boldsymbol{\Psi}}\in\mathbb{S}^l \end{aligned}$$

S-MLE-PL (sequential)

$$\begin{aligned} &\underset{\boldsymbol{\gamma},\gamma_l,w_{\theta_l},\{\tau_i\}_{i=1}^{n}}{\text{minimize}} && \mathcal{L}(\widetilde{\boldsymbol{x}}^i;\boldsymbol{\gamma},\gamma_l,w_{\theta_l},\{\tau_i\}_{i=1}^{n}) \\ &\text{subject to} && \theta_1=0,\ |w_{\theta_l}|=1,\ \boldsymbol{\gamma},\gamma_l\ \text{real} \end{aligned}$$

w_{θ_l} is estimated with :

- estimated past
  - $\hat{w}_\theta$
  - $\hat{\boldsymbol{\Sigma}}$
- new data

statistics of the conditional distribution of new image with respect to the past

$$\begin{aligned} &\mathcal{L}(\widetilde{\boldsymbol{x}}^i;\boldsymbol{\gamma},\gamma_l,w_{\theta_l},\{\tau_i\}_{i=1}^{n}) \\ &= -\sum_{i=1}^{n}\mathcal{L}^i(x_l^i|\boldsymbol{x}^i;\boldsymbol{\gamma},\gamma_l,w_{\theta_l},\{\tau_i\}_{i=1}^{n}) \\ &\quad+\mathcal{L}^i(\boldsymbol{x}^i;\{\tau_i\}_{i=1}^{n}) \end{aligned}$$

According to [2], $x_l^i|\boldsymbol{x}^i\sim\mathcal{CN}(\mu_x^i,\sigma_x^2)$ where

- $\mu_x^i=w_{\theta_l}\boldsymbol{\gamma}\text{diag}(\hat{\boldsymbol{w}}_{\boldsymbol{\theta}})^H\hat{\Sigma}^{-1}\boldsymbol{x}^i$
- $\sigma_x^2=\gamma_l-\boldsymbol{\gamma}\text{diag}(\hat{\boldsymbol{w}}_{\boldsymbol{\theta}})^H\hat{\Sigma}^{-1}\text{diag}(\hat{\boldsymbol{w}}_{\boldsymbol{\theta}}^H)\boldsymbol{\gamma}^T$

[2] T.W. Anderson (1962) "An introduction to multivariate statistical analysis".

MLE problem

$$\begin{array}{ll} \underset{\boldsymbol{\gamma},\gamma_l,w_{\theta_l},\{\tau_i\}_{i=1}^n}{\text{minimize}} & \mathcal{L}(\widetilde{\boldsymbol{x}}^i;\boldsymbol{\gamma},\gamma_l,w_{\theta_l},\{\tau_i\}_{i=1}^n) \\ \text{subject to} & \theta_1=0,\ |w_{\theta_l}|=1,\ \boldsymbol{\gamma},\gamma_l \text{ real} \end{array}$$

MLE problem

$$
\begin{aligned}
\underset{\boldsymbol{\gamma},\gamma_l,w_{\theta_l},\{\tau_i\}_{i=1}^n}{\text{minimize}} \quad & \mathcal{L}(\widetilde{\mathbf{x}}^i;\boldsymbol{\gamma},\gamma_l,w_{\theta_l},\{\tau_i\}_{i=1}^n) \\
\text{subject to} \quad & \theta_1 = 0, |w_{\theta_l}| = 1, \boldsymbol{\gamma},\gamma_l \text{ real}
\end{aligned}
$$

Bloc 1

Update $\{\tau_i\}_{i=1}^n$:
Minimize $\mathcal{L}$ *with fixed* $\boldsymbol{\gamma}$ *and* γ_0 *and* w_{θ_l}

↓

Bloc 2

Update $\boldsymbol{\gamma}$:
Minimize $\mathcal{L}$ *with fixed* γ_0, w_{θ_l} *and* $\{\tau_i\}_{i=1}^n$

↓

Bloc 3

Update γ_0:
Minimize $\mathcal{L}$ *with fixed* $\boldsymbol{\gamma}$, w_{θ_l} *and* $\{\tau_i\}_{i=1}^n$

↓

Bloc 4

Update w_{θ_l} :
Minimize $\mathcal{L}$ *with fixed* γ_0, $\boldsymbol{\gamma}$ *and* $\{\tau_i\}_{i=1}^n$

n_{iter}
BCD

MLE problem

$$\begin{array}{ll} \underset{\widetilde{\boldsymbol{\Psi}}, \widetilde{\boldsymbol{w}}_{\boldsymbol{\theta}}, \{\tau_i\}_{i=1}^n}{\text{minimize}} & \mathcal{L}(\widetilde{\mathbf{x}}^i; \widetilde{\boldsymbol{\Psi}}, \widetilde{\boldsymbol{w}}_{\boldsymbol{\theta}}, \{\tau_i\}_{i=1}^n) \\ \text{subject to} & \theta_1 = 0, \widetilde{\boldsymbol{w}}_{\boldsymbol{\theta}} \in \mathbb{T}_l, \widetilde{\boldsymbol{\Psi}} \in \mathbb{S}^l \end{array}$$

$$\begin{array}{ll} \underset{\boldsymbol{\gamma}, \gamma_l, w_{\theta_l}, \{\tau_i\}_{i=1}^n}{\text{minimize}} & \mathcal{L}(\widetilde{\mathbf{x}}^i; \boldsymbol{\gamma}, \gamma_l, w_{\theta_l}, \{\tau_i\}_{i=1}^n) \\ \text{subject to} & \theta_1 = 0, |w_{\theta_l}| = 1, \boldsymbol{\gamma}, \gamma_l \text{ real} \end{array}$$

Bloc 1

Update $\{\tau_i\}_{i=1}^n$:
Minimize $\mathcal{L}$ *with fixed* $\widetilde{\boldsymbol{w}}_\theta$ *and* $\widetilde{\boldsymbol{\Psi}}$

Bloc 2

Update $\widetilde{\boldsymbol{\Psi}}$:
Minimize $\mathcal{L}$ *with fixed* $\widetilde{\mathbf{w}}_\theta$ *and* $\{\tau_i\}_{i=1}^n$

Bloc 3

Update $\widetilde{\mathbf{w}}_\theta$:
Minimize $\mathcal{L}$ *with fixed* $\widetilde{\boldsymbol{\Psi}}$ *and* $\{\tau_i\}_{i=1}^n$

n_{iter} *MM*

n_{iter} *BCD*

complexity: $O(l^3)$

Bloc 1

Update $\{\tau_i\}_{i=1}^n$:
Minimize $\mathcal{L}$ *with fixed* $\boldsymbol{\gamma}$ *and* $\gamma_{\mathbf{0}}$ *and* w_{θ_l}

Bloc 2

Update $\boldsymbol{\gamma}$:
Minimize $\mathcal{L}$ *with fixed* $\gamma_{\mathbf{0}}$, w_{θ_l} *and* $\{\tau_i\}_{i=1}^n$

Bloc 3

Update $\gamma_{\mathbf{0}}$:
Minimize $\mathcal{L}$ *with fixed* $\boldsymbol{\gamma}$, w_{θ_l} *and* $\{\tau_i\}_{i=1}^n$

Bloc 4

Update w_{θ_l} :
Minimize $\mathcal{L}$ *with fixed* $\gamma_{\mathbf{0}}$, $\boldsymbol{\gamma}$ *and* $\{\tau_i\}_{i=1}^n$

n_{iter} *BCD*

complexity: $O(p^2)$ with $l > p$

Testing our algorithms on real data

Mexico City

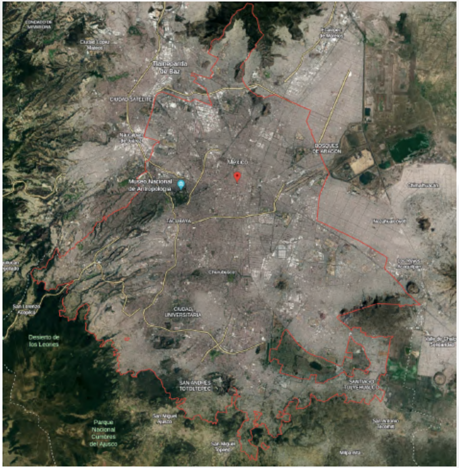

Hawaï Island

Testing our algorithms on real data

Mexico City

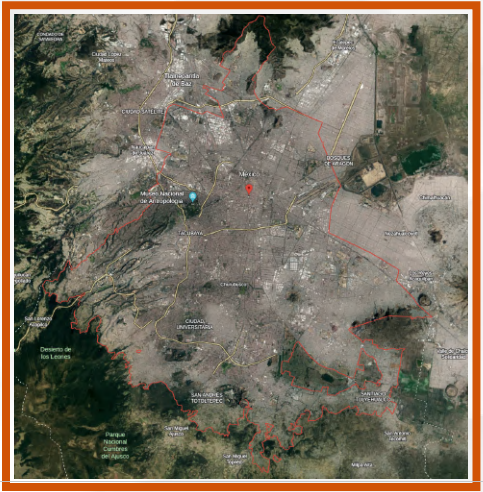

Hawaï Island

Study Area: Mexico City

Figure: Mexico City (source : Google Earth)

Study area context

- One of the most densely populated urban areas> 20M
- Population grew from **3 M** (1950) to **22.7 M** (2025)
- **Rapid urbanization ⇒ groundwater extraction ⇒ land subsidence**

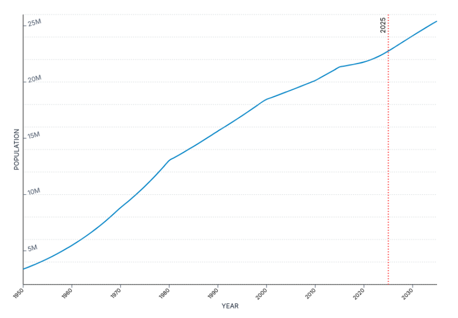

Figure: Evolution of Mexico City's population (source : World Population Reviews)

Dataset

General Information:

- **Sensor:** Sentinel-1 (C-band)
- **Acquisition mode:** Interferometric Wide Swath (IW)
- **Orbit direction:** Descending
- **Polarization:** VV
- **Path / Frame:** 143 / 526

Temporal Coverage:

- **Number of images:** 40
- **Time span:** August 14, 2019 – December 6, 2020
- **Total duration:** 480 days ($\approx$ 1.3 years)
- **Temporal interval:** 12 days

GPS Data:

- **Stations:** ICMX, UNVA, MMX1 (temporally and spatially aligned with the SAR dataset)
- **Measurements:** 3D displacements (East, North, Up)

Figure: Map of the available Global Positioning System (GPS)

Results on Real Data: Mexico City

We evaluate the proposed method using a real dataset of Mexico City. The dataset consists of **20 satellite images** acquired between **August 14, 2019** and **April 10, 2020** with a spatial window of size 7×7 pixels.

Methods and input data:

- **S-MLE-PL**: uses $p = 19$ historical images and one new image.
- **MLE-PL** [6]: uses all $l = 20$ available images.
- **SE** [4]: uses a temporal sliding window of size $s = 5$ images.

[6] P.V.H. Vu et al. (2023) "Robust Phase Linking in InSAR".
[4] H. Ansari et al. (2017) "Sequential Estimator: Toward efficient InSAR time series analysis".

Results on real data: Mexico City

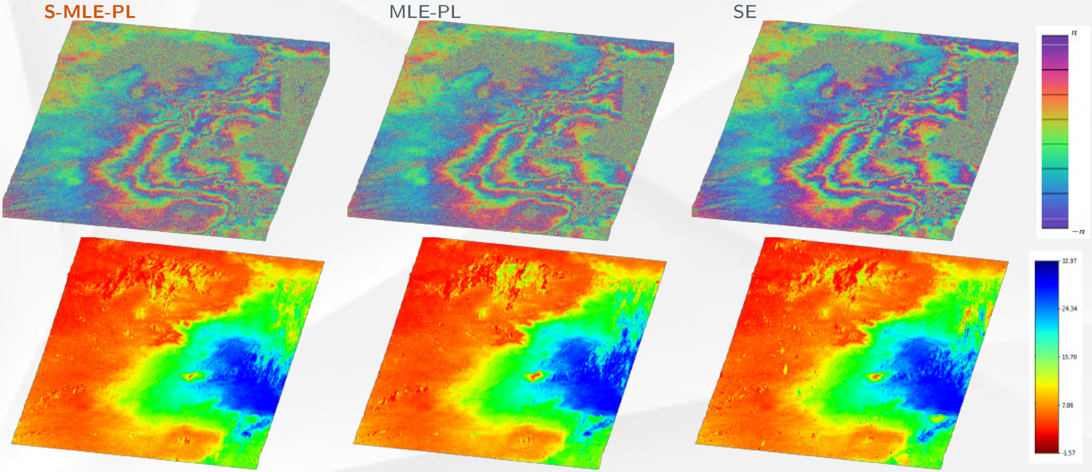

Figure: Close-up view of the wrapped and the unwrapped interferograms (14 August 2019 - 10 April 2020) estimated by S-MLE-PL ($p+1=20$), MLE-PL [6] and SE [4] ($s=5$) with a spatial window of size $n = 7 \times 7$.

Results on real data: Mexico City

	RMSE (↓)	SSIM (↑)	Colinearity (↑) [3]	computation time
MLE-PL [6]	Ref	Ref	0.61	38.4 min
S-MLE-PL	2.87	0.70	0.57	4.72 min
SE [4]	2.96	0.67	0.76	16.97 min

Table: Quantitative comparison between the **S-MLE-PL**, MLE-PL [6], and SE [4] approaches.

[6] P.V.H. Vu et al. (2023) "Robust Phase Linking in InSAR".
[4] H. Ansari et al. (2017) "Sequential Estimator: Toward efficient InSAR time series analysis".
[3] B. Pinel-Puysségur et al. (2012) "Multi-link InSAR timeseries: Enhancement of a wrapped interferometric database".

Content

Data Model

Limitations:

- S-MLE-PL adds one image at a time, limiting multi-image information.
- S-MLE-PL does not allow the direct use of regularization techniques.

$\Longrightarrow$ **We introduce S-COFI-PL approach**

Data Model

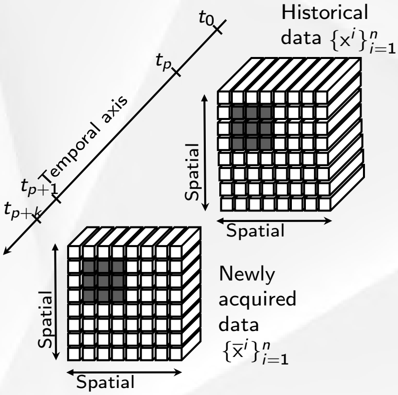

Figure: Representation of a SAR time series using a sliding window of n pixels $\widetilde{\mathrm{x}}^i$.

Limitations:

- S-MLE-PL adds one image at a time, limiting multi-image information.
- S-MLE-PL does not allow the direct use of regularization techniques.

$\Longrightarrow$ **We introduce S-COFI-PL approach**

We consider a set $\{\widetilde{\mathrm{x}}^i\}_{i=1}^n$, where

$$\widetilde{\mathrm{x}}^i = [\underbrace{x_1^i, \ldots, x_p^i}_{\mathrm{x}^i}, \underbrace{x_{p+1}^i, \ldots, x_{p+k}^i}_{\overline{\mathrm{x}}^i}]^T \in \mathbb{C}^{p+k}$$

Each pixel is assumed i.i.d. and follows a zero-mean CCG distribution: $\widetilde{\mathrm{x}} \sim \mathcal{CN}(0, \widetilde{\Sigma})$.

$$\widetilde{\Sigma} = \begin{pmatrix} \Sigma_p & (\Sigma_{pn})^H \\ \Sigma_{pn} & \Sigma_n \end{pmatrix} \qquad \widetilde{\boldsymbol{w}}_\theta = \begin{pmatrix} \boldsymbol{w}_\theta \\ \overline{\boldsymbol{w}}_\theta \end{pmatrix}$$

Problem reformulation

$$\begin{aligned} \underset{\overline{\mathbf{w}}_{\boldsymbol{\theta}}}{\text{minimize}} \quad & f^{\mathrm{d}}_{\widetilde{\Sigma}}\left(\widetilde{\Sigma}, \widetilde{\Psi} \circ \widetilde{\mathrm{w}}_{\theta}\widetilde{\mathrm{w}}_{\theta}^{H}\right) \\ \text{subject to} \quad & \theta_1 = 0 \\ & \overline{\mathbf{w}}_{\boldsymbol{\theta}} \in \mathbb{T}_k \end{aligned}$$

Problem reformulation

$$\begin{array}{ll} \underset{\overline{\mathbf{w}}_{\boldsymbol{\theta}}}{\text{minimize}} & f^{\mathrm{d}}_{\widetilde{\Sigma}}\left(\widetilde{\Sigma}, \widetilde{\Psi} \circ \widetilde{\mathrm{w}}_\theta \widetilde{\mathrm{w}}_\theta^H\right) \\ \text{subject to} & \theta_1 = 0 \\ & \overline{\mathbf{w}}_{\boldsymbol{\theta}} \in \mathbb{T}_k \end{array}$$

Covariance matrix plug-in

- SCM: $\widetilde{\Sigma}^U = \frac{1}{n}\sum_{i=1}^n \widetilde{\mathrm{x}}^i \widetilde{\mathrm{x}}^{iH}$
- PO: $\widetilde{\Sigma}^U = \frac{1}{n}\sum_{i=1}^n \widetilde{\mathrm{y}}^i \widetilde{\mathrm{y}}^{iH}$ where $\widetilde{\mathrm{y}} = \Phi_{\mathbb{T}}(\widetilde{\mathrm{x}})$ and $\Phi : \gamma e^{j\theta} \to e^{j\theta}$
- ...

+ Regularization

- Shrinkage to identity: $\widetilde{\Sigma}^{SK} = \beta\widetilde{\Sigma}^U + (1-\beta)\frac{\mathrm{tr}(\widetilde{\Sigma}^U)}{p+k}\mathrm{I}_{p+k}$
- Tapering: $\widetilde{\Sigma}^{BW} = \mathrm{W}(b) \circ \widetilde{\Sigma}^U$ with $[\mathrm{W}(b)]_{ij} = \begin{cases} 1 & \text{if } \; |i-j| \leq b \\ 0 & \text{otherwise} \end{cases}$
- ...

Problem reformulation

$$
\begin{aligned}
\underset{\overline{\mathbf{w}}_{\boldsymbol{\theta}}}{\text{minimize}} \quad & f^{\mathrm{d}}_{\widetilde{\Sigma}}\left(\widetilde{\Sigma}, \widetilde{\Psi} \circ \widetilde{\mathrm{w}}_\theta \widetilde{\mathrm{w}}_\theta^H\right) \\
\text{subject to} \quad & \theta_1 = 0 \\
& \overline{\mathbf{w}}_{\boldsymbol{\theta}} \in \mathbb{T}_k
\end{aligned}
$$

Covariance matrix plug-in

- SCM: $\widetilde{\Sigma}^U = \frac{1}{n} \sum_{i=1}^n \widetilde{\mathrm{x}}^i \widetilde{\mathrm{x}}^{iH}$
- PO: $\widetilde{\Sigma}^U = \frac{1}{n} \sum_{i=1}^n \widetilde{\mathrm{y}}^i \widetilde{\mathrm{y}}^{iH}$ where $\widetilde{\mathrm{y}} = \Phi_{\mathbb{T}}(\widetilde{\mathrm{x}})$ and $\Phi : \gamma e^{j\theta} \to e^{j\theta}$
- ...

+ Regularization

- Shrinkage to identity: $\widetilde{\Sigma}^{SK} = \beta \widetilde{\Sigma}^U + (1-\beta) \frac{\mathrm{tr}(\widetilde{\Sigma}^U)}{p+k} \mathrm{I}_{p+k}$
- Tapering: $\widetilde{\Sigma}^{BW} = \mathrm{W}(b) \circ \widetilde{\Sigma}^U$ with $[\mathrm{W}(b)]_{ij} = \begin{cases} 1 & \text{if } \quad |i-j| \leq b \\ 0 & \text{otherwise} \end{cases}$
- ...

Matrix distances

- Kullback-Leibler (KL) divergence:

$$f^{\mathrm{KL}}_{\widetilde{\Sigma}}(\widetilde{\mathrm{w}}_{\boldsymbol{\theta}}) = \widetilde{\mathrm{w}}_{\boldsymbol{\theta}}^H (\widetilde{\Psi}^{-1} \circ \widetilde{\Sigma}) \widetilde{\mathrm{w}}_{\boldsymbol{\theta}}$$

- Frobenius norm (FN):

$$f^{\mathrm{FN}}_{\widetilde{\Sigma}}(\widetilde{\mathrm{w}}_{\boldsymbol{\theta}}) = -2 \widetilde{\mathrm{w}}_{\boldsymbol{\theta}}^H (\widetilde{\Psi} \circ \widetilde{\Sigma}) \widetilde{\mathrm{w}}_{\boldsymbol{\theta}}$$

- ...

Optimization problem resolution - MM algorithm (1/2)

S-COFI-PL optimization problem

$\longrightarrow$ no analytical solution

$\longrightarrow$ iterative algorithm

S-COFI-PL

$$\begin{array}{ll} \underset{\overline{\mathbf{w}}_{\boldsymbol{\theta}}}{\text{minimize}} & f^{\mathrm{d}}_{\widetilde{\Sigma}}\left(\widetilde{\Sigma},\ \widetilde{\Psi} \circ \widetilde{\mathbf{w}}_{\theta}\widetilde{\mathbf{w}}_{\theta}^{H}\right) \\ \text{subject to} & \overline{\mathbf{w}}_{\boldsymbol{\theta}} \in \mathbb{T}_k, \\ & \theta_1 = 0 \end{array}$$

[10] Y. Sun et al. (2016) "Majorization-Minimization algorithms in signal processing, communications, and Machine Learning".

Optimization problem resolution - MM algorithm (1/2)

S-COFI-PL optimization problem

$\longrightarrow$ no analytical solution

$\longrightarrow$ iterative algorithm

S-COFI-PL

$$\begin{aligned} \underset{\overline{\mathbf{w}}_{\boldsymbol{\theta}}}{\text{minimize}} \quad & f^{d}_{\widetilde{\Sigma}}\left(\widetilde{\Sigma}, \widetilde{\Psi} \circ \widetilde{\mathbf{w}}_{\theta}\widetilde{\mathbf{w}}_{\theta}^{H}\right) \\ \text{subject to} \quad & \overline{\mathbf{w}}_{\boldsymbol{\theta}} \in \mathbb{T}_k, \\ & \theta_1 = 0 \end{aligned}$$

$$\underset{x \in \mathcal{X}}{\text{minimize}} \quad f(x)$$

Majorization-Minimization (MM) algorithm [10]:

- **step 1:** majorizing the cost function by a $g(.|x_t)$: $f(x) \leq g(x|x_t)$
- **step 2:** minimizing the obtained function $g(x|x_t)$

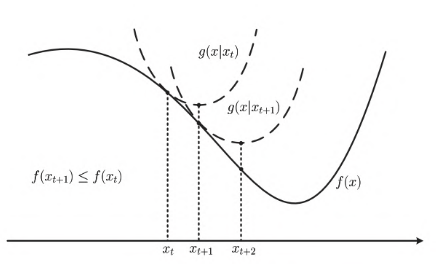

[10] Y. Sun et al. (2016) "Majorization-Minimization algorithms in signal processing, communications, and Machine Learning".

Optimization problem resolution - MM algorithm (2/2)

step1:

Lemma The concave quadratic form $f : \mathrm{w} \longrightarrow -\mathrm{w}^H \mathrm{H} \mathrm{w}$ is majorized by $-\mathrm{Re}(\mathrm{w}^H \mathrm{H} \mathrm{w}^{(t)})$ with equality at point $\mathrm{w}^{(t)}$.

$$f_{\widetilde{\Sigma}}^{\mathrm{FN}}(\widetilde{\mathrm{w}}_{\theta}) = -2\mathrm{w}_{\theta}^H(|\Sigma_p| \circ \Sigma_p)\mathrm{w}_{\theta} - 2\mathrm{w}_{\theta}^H(|\Sigma_{pn}|)^T \circ (\Sigma_{pn})^H)\overline{\boldsymbol{w}}_{\boldsymbol{\theta}} - 2\overline{\boldsymbol{w}}_{\boldsymbol{\theta}}{}^H(|\Sigma_{pn}| \circ \Sigma_{pn})\mathrm{w}_{\theta} - 2\overline{\boldsymbol{w}}_{\boldsymbol{\theta}}{}^H(|\Sigma_n| \circ \Sigma_n)\overline{\boldsymbol{w}}_{\boldsymbol{\theta}}$$

is majorized by the following expression

$$g(\overline{\boldsymbol{w}}_{\boldsymbol{\theta}}|\overline{\boldsymbol{w}}_{\boldsymbol{\theta}}^{(t)}) = -\mathrm{Re}\left(\overline{\boldsymbol{w}}_{\boldsymbol{\theta}}{}^H \cdot 4\left[(|\Sigma_{pn}| \circ \Sigma_{pn})\mathrm{w}_{\theta} + (|\Sigma_n| \circ \Sigma_n)\overline{\boldsymbol{w}}_{\boldsymbol{\theta}}^{(t)}\right]\right)$$

Optimization problem resolution - MM algorithm (2/2)

step1:

Lemma The concave quadratic form $f : \mathrm{w} \longrightarrow -\mathrm{w}^H \mathrm{H}\mathrm{w}$ is majorized by $-\mathrm{Re}(\mathrm{w}^H \mathrm{H}\mathrm{w}^{(t)})$ with equality at point $\mathrm{w}^{(t)}$.

$$f_{\tilde{\Sigma}}^{\mathrm{FN}}(\widetilde{\mathrm{w}}_\theta) = -2\mathrm{w}_\theta^H(|\Sigma_p| \circ \Sigma_p)\mathrm{w}_\theta - 2\mathrm{w}_\theta^H(|\Sigma_{pn}|)^T \circ (\Sigma_{pn})^H)\overline{\boldsymbol{w}}_\theta - 2\overline{\boldsymbol{w}}_\theta{}^H(|\Sigma_{pn}| \circ \Sigma_{pn})\mathrm{w}_\theta - 2\overline{\boldsymbol{w}}_\theta{}^H(|\Sigma_n| \circ \Sigma_n)\overline{\boldsymbol{w}}_\theta$$

is majorized by the following expression

$$g(\overline{\boldsymbol{w}}_\theta|\overline{\boldsymbol{w}}_\theta^{(t)}) = -\mathrm{Re}\left(\overline{\boldsymbol{w}}_\theta{}^H \cdot 4\left[(|\Sigma_{pn}| \circ \Sigma_{pn})\mathrm{w}_\theta + (|\Sigma_n| \circ \Sigma_n)\overline{\boldsymbol{w}}_\theta^{(t)}\right]\right)$$

step 2:

Lemma The solution of the minimization problem $\min_{\mathrm{w}\in\mathbb{T}_k} -\mathrm{Re}(\mathrm{w}^H \breve{\boldsymbol{w}}^{(t)})$ is obtained as $\mathrm{w}^* = \Phi_{\mathbb{T}}(\breve{\boldsymbol{w}}^{(t)})$ with $\Phi_{\mathbb{T}} : x = re^{i\theta} \rightarrow e^{i\theta}$

The problem is equivalent to

$$\min_{\overline{\boldsymbol{w}}_\theta \in\mathbb{T}_k} -\mathrm{Re}\left(\overline{\boldsymbol{w}}_\theta{}^H \cdot \underbrace{4\left[(|\Sigma_{pn}| \circ \Sigma_{pn})\mathrm{w}_\theta + (|\Sigma_n| \circ \Sigma_n)\overline{\boldsymbol{w}}_\theta^{(t)}\right]}_{\breve{\boldsymbol{w}}_\theta^{(t)}}\right)$$

and the solution is obtained as $\overline{\boldsymbol{w}}_\theta^{(t+1)} = \Phi_{\mathbb{T}}(\breve{\boldsymbol{w}}_\theta^{(t)})$

Results on Real Data: Mexico City

We evaluate the proposed method using a real dataset of Mexico City. The dataset consists of **40 satellite images** acquired between **August 14, 2019** and **December 6, 2020** with a spatial window of size 7×7 pixels.

Methods and input data:

- **S-COFI-PL**: uses $p = 35$ historical images and $k = 5$ new images.
- **COFI-PL** [7]: uses all $l = 40$ available images.
- **SE** [4]: uses a temporal sliding window of size $s = 5$ images.

[7] P.V.H. Vu et al. (2025) "Covariance Fitting Interferometric Phase Linking: Modular Framework and Optimization Algorithms".
[4] H. Ansari et al. (2017) "Sequential Estimator: Toward efficient InSAR time series analysis".

Results on real data: Mexico City

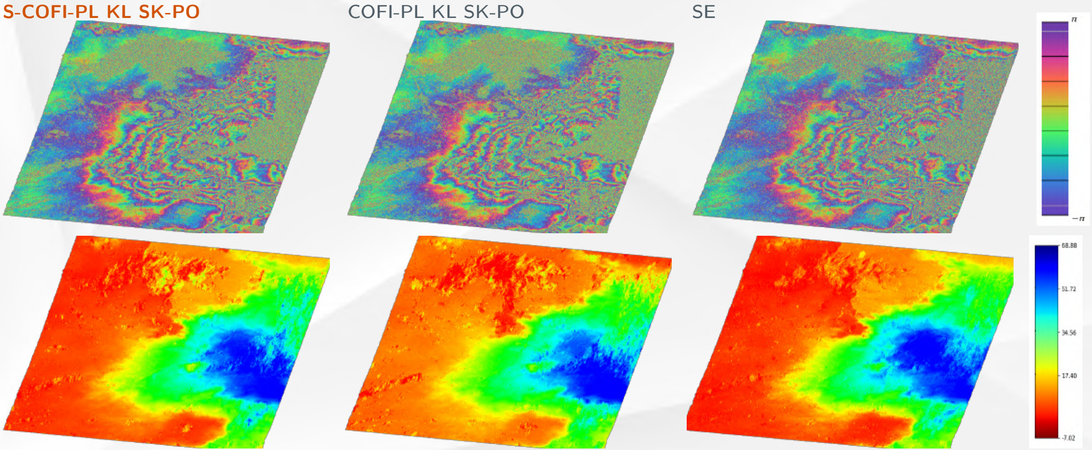

Figure: Close-up view of the wrapped and the unwrapped interferogram (14 August 2019 - 6 December 2020) estimated by S-COFI-PL and COFI-PL [7] using KL divergence and SK-PO and by SE [4].

Results on real data: Mexico City

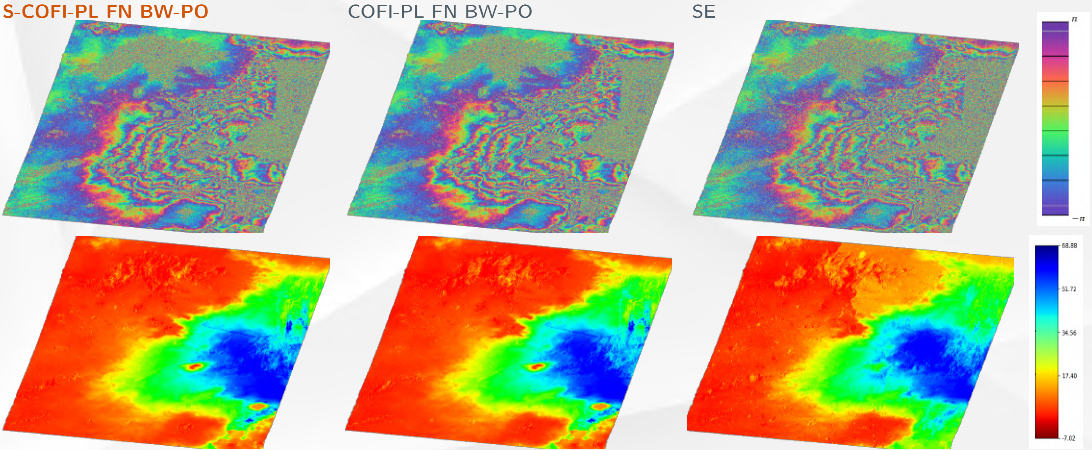

Figure: Close-up view of the wrapped and the unwrapped interferogram (14 August 2019 - 6 December 2020) estimated,by S-COFI-PL and COFI-PL [7] using FN and BW-PO, and by SE [4].

Results on real data: Mexico City

		RMSE (↓)	SSIM (↑)	Colinearity [3] (↑)	computation time
KL	S-COFI-PL	7.54	0.62	**0.64**	**0.44**h
SK-PO	COFI-PL [7]	7.73	0.55	0.60	0.52h
FN	S-COFI-PL	**2.07**	**0.89**	**0.89**	**0.37**h
BW-PO	COFI-PL [7]	Ref	Ref	**0.89**	0.43h
	SE [4]	7.47	0.24	0.72	0.5h

Table: Comparison of COFI-PL [7] and **S-COFI-PL** and SE [4].

Recap

KL : Kullback-Leibler divergence

BW : banding

PO : Phase-Only

FN : Frobenius Norm

SK : Shrinkage-to-identity

[7] P.V.H. Vu et al. (2025) "Covariance Fitting Interferometric Phase Linking: Modular Framework and Optimization Algorithms".
[4] H. Ansari et al. (2017) "Sequential Estimator: Toward efficient InSAR time series analysis".
[3] B. Pinel-Puysségur et al. (2012) "Multi-link InSAR timeseries: Enhancement of a wrapped interferometric database".

Content

Data model

Limitations:

- S-MLE-PL and S-COFI-PL require storing and processing all historical images.
- This increases memory and computation requirements.

$\Longrightarrow$ **We introduce SI-IPL approach**

Data model

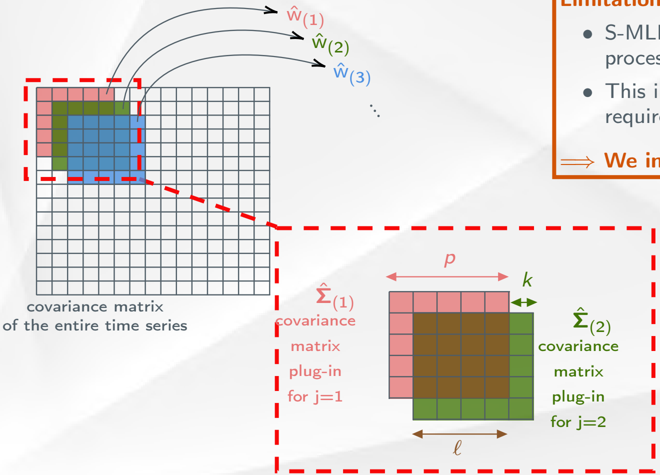

Limitations:

- S-MLE-PL and S-COFI-PL require storing and processing all historical images.
- This increases memory and computation requirements.

$\Longrightarrow$ **We introduce SI-IPL approach**

- p: size of the temporal window
- k: size of the stride or the new added images
- $\ell = p - k$: size of the overlap

Optimization problem

COFI-PL (offline)

$$\begin{aligned} \underset{\tilde{\boldsymbol{w}}_{\boldsymbol{\theta}}}{\text{minimize}} \quad & f^{FN}_{\tilde{\boldsymbol{\Sigma}}}(\tilde{\boldsymbol{\Sigma}}, \tilde{\boldsymbol{\Psi}} \circ \tilde{\boldsymbol{w}}_{\boldsymbol{\theta}} \tilde{\boldsymbol{w}}_{\boldsymbol{\theta}}^H) \\ \text{subject to} \quad & \theta_1 = 0 \\ & \tilde{\boldsymbol{w}}_{\boldsymbol{\theta}} \in \mathbb{T}_l \end{aligned}$$

[7] P.V.H. Vu et al. (2025) "Covariance Fitting Interferometric Phase Linking: Modular Framework and Optimization Algorithms".

Optimization problem

COFI-PL (offline)

$$\begin{aligned} \underset{\widetilde{\boldsymbol{w}}_{\boldsymbol{\theta}}}{\text{minimize}} \quad & f^{FN}_{\widetilde{\boldsymbol{\Sigma}}}(\widetilde{\boldsymbol{\Sigma}}, \widetilde{\boldsymbol{\Psi}} \circ \widetilde{\boldsymbol{w}}_{\boldsymbol{\theta}} \widetilde{\boldsymbol{w}}_{\boldsymbol{\theta}}{}^{H}) \\ \text{subject to} \quad & \theta_1 = 0 \\ & \widetilde{\boldsymbol{w}}_{\boldsymbol{\theta}} \in \mathbb{T}_l \end{aligned}$$

SI-IPL (sequential)

$$\begin{aligned} \underset{\mathbf{w}_{(j)}}{\text{minimize}} \quad & f^{FN}_{\hat{\boldsymbol{\Sigma}}_{(j)}}(\boldsymbol{\Sigma}_{(j)}, \boldsymbol{\Psi}_{(j)} \circ \mathbf{w}_{(j)} \mathbf{w}_{(j)}{}^{H}) \\ & + \lambda h(\mathbf{w}_{(j)}) \\ \text{subject to} \quad & \mathbf{w}_{(j)} \in \mathbb{T}_p \end{aligned}$$

$$h(\mathbf{w}_{(j)}) = \left\| \begin{pmatrix} \mathbf{w}_{\ell(j-1)} \\ 0 \end{pmatrix} - \mathbf{w}_{(j)} \right\|^2$$

[7] P.V.H. Vu et al. (2025) "Covariance Fitting Interferometric Phase Linking: Modular Framework and Optimization Algorithms".

Optimization problem

COFI-PL (offline)

$$\begin{array}{ll} \underset{\widetilde{\boldsymbol{w}}_{\boldsymbol{\theta}}}{\text{minimize}} & f^{FN}_{\widetilde{\boldsymbol{\Sigma}}}(\widetilde{\boldsymbol{\Sigma}}, \widetilde{\boldsymbol{\Psi}} \circ \widetilde{\boldsymbol{w}}_{\boldsymbol{\theta}} \widetilde{\boldsymbol{w}}_{\boldsymbol{\theta}}^H) \\ \text{subject to} & \theta_1 = 0 \\ & \widetilde{\boldsymbol{w}}_{\boldsymbol{\theta}} \in \mathbb{T}_l \end{array}$$

SI-IPL (sequential)

$$\begin{array}{ll} \underset{\mathrm{w}_{(j)}}{\text{minimize}} & f^{FN}_{\hat{\boldsymbol{\Sigma}}_{(j)}}(\boldsymbol{\Sigma}_{(j)}, \boldsymbol{\Psi}_{(j)} \circ \mathrm{w}_{(j)} \mathrm{w}_{(j)}^H) \\ & +\lambda h(\mathrm{w}_{(j)}) \\ \text{subject to} & \mathrm{w}_{(j)} \in \mathbb{T}_p \end{array}$$

$$h(\mathrm{w}_{(j)}) = \left\| \begin{pmatrix} \mathrm{w}_{\ell(j-1)} \\ 0 \end{pmatrix} - \mathrm{w}_{(j)} \right\|^2$$

Algorithm MM algorithm for SI-IPL

Input: $\hat{\boldsymbol{\Sigma}}_{(j)} \in \mathbb{C}^{p \times p}$

Compute : $\mathrm{M} = 4(|\hat{\boldsymbol{\Sigma}}_{(j)}| \circ \hat{\boldsymbol{\Sigma}}_{(j)})$

repeat

$\ddot{\mathrm{w}}^{(t)}_{(j)} = \mathrm{M}\mathrm{w}_{(j)} + 2\lambda \begin{pmatrix} \mathrm{w}_{\ell(j-1)} \\ 0 \end{pmatrix}$

$\mathrm{w}^{(t)}_{(j)} = \Phi_{\mathbb{T}}\{\ddot{\mathrm{w}}^{(t)}_{(j)}\}$

$t = t + 1$

until convergence

Output: $\hat{\mathrm{w}}_{(j)} = \mathrm{w}_{end} \in \mathbb{T}_p$

[7] P.V.H. Vu et al. (2025) "Covariance Fitting Interferometric Phase Linking: Modular Framework and Optimization Algorithms".

Optimization problem

COFI-PL (offline)

$$\begin{aligned} \underset{\tilde{\boldsymbol{w}}_{\boldsymbol{\theta}}}{\text{minimize}} \quad & f^{FN}_{\tilde{\boldsymbol{\Sigma}}}(\tilde{\boldsymbol{\Sigma}}, \tilde{\boldsymbol{\Psi}} \circ \tilde{\boldsymbol{w}}_{\boldsymbol{\theta}} \tilde{\boldsymbol{w}}_{\boldsymbol{\theta}}^H) \\ \text{subject to} \quad & \theta_1 = 0 \\ & \tilde{\boldsymbol{w}}_{\boldsymbol{\theta}} \in \mathbb{T}_l \end{aligned}$$

SI-IPL (sequential)

$$\begin{aligned} \underset{\mathbf{w}_{(j)}}{\text{minimize}} \quad & f^{FN}_{\hat{\boldsymbol{\Sigma}}_{(j)}}(\boldsymbol{\Sigma}_{(j)}, \boldsymbol{\Psi}_{(j)} \circ \mathbf{w}_{(j)} \mathbf{w}_{(j)}^H) \\ & + \lambda h(\mathbf{w}_{(j)}) \\ \text{subject to} \quad & \mathbf{w}_{(j)} \in \mathbb{T}_p \end{aligned}$$

$$h(\mathbf{w}_{(j)}) = \left\| \begin{pmatrix} \mathbf{w}_{\ell(j-1)} \\ 0 \end{pmatrix} - \mathbf{w}_{(j)} \right\|^2$$

Algorithm MM algorithm for SI-IPL

Input: $\hat{\boldsymbol{\Sigma}}_{(j)} \in \mathbb{C}^{p \times p}$

Compute : $\mathrm{M} = 4(|\hat{\boldsymbol{\Sigma}}_{(j)}| \circ \hat{\boldsymbol{\Sigma}}_{(j)})$

repeat

$\ddot{\mathbf{w}}^{(t)}_{(j)} = \mathrm{M}\mathbf{w}_{(j)} + 2\lambda \begin{pmatrix} \mathbf{w}_{\ell(j-1)} \\ 0 \end{pmatrix}$

$\mathbf{w}^{(t)}_{(j)} = \Phi_{\mathbb{T}}\{\ddot{\mathbf{w}}^{(t)}_{(j)}\}$

$t = t + 1$

until convergence

Output: $\hat{\mathbf{w}}_{(j)} = \mathbf{w}_{end} \in \mathbb{T}_p$

method	complexity
SI-IPL	$O(p^2)$
COFI-PL [7]	$O(l^2)$

with $l > p$.

[7] P.V.H. Vu et al. (2025) "Covariance Fitting Interferometric Phase Linking: Modular Framework and Optimization Algorithms".

Results on Real Data: Mexico City

We evaluate the proposed method using a real dataset of Mexico City. The dataset consists of **30 satellite images** acquired between **August 14, 2019** and **July 16, 2020** with a spatial window of size 7×7 pixels.

Methods and input data:

- **SI-IPL**: uses $p = 5$, $\ell = 4$, and $k = 1$.
- **COFI-PL** [7]: uses all $l = 30$ available images.
- **SE** [4]: uses a temporal sliding window of size $s = 5$ images.

[7] P.V.H. Vu et al. (2025) "Covariance Fitting Interferometric Phase Linking: Modular Framework and Optimization Algorithms".
[4] H. Ansari et al. (2017) "Sequential Estimator: Toward efficient InSAR time series analysis".

Results on real data: Mexico City

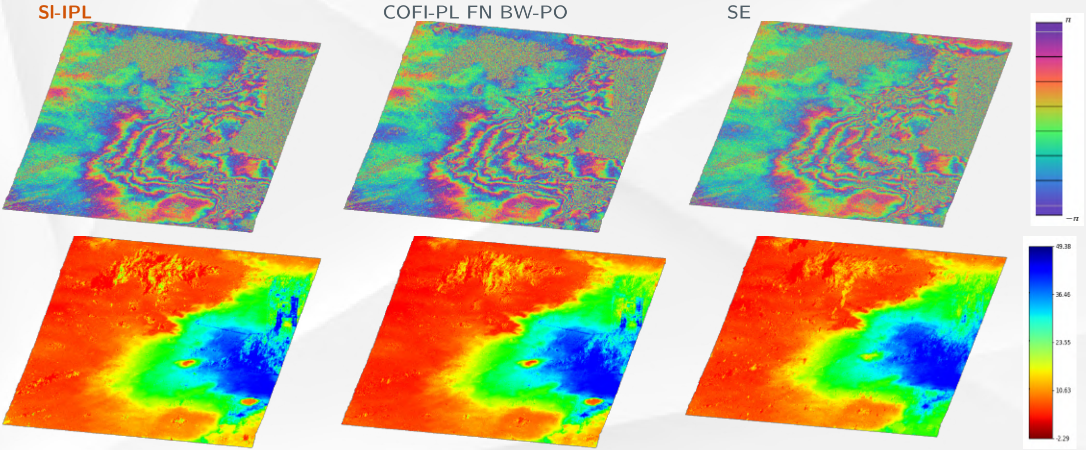

Figure: Close-up view of the wrapped and the unwrapped interferogram estimated by SI-IPL, COFI-PL [7] and SE [4].

Results on real data: Mexico City

method	colinearity [3] (↑)	SSIM (↑)	time
COFI-PL [7]	**0.91**	Ref	19.35 min
SI-IPL	**0.90**	**0.94**	**3.9** min
SE [4]	0.84	0.85	17.1 min

Table: Quantitative values for the evaluation of the estimated phases of **SI-IPL**, the SE [4] and COFI-PL [7].

[3] B. Pinel-Puysségur et al. (2012) "Multi-link InSAR time series: Enhancement of a wrapped interferometric database".
[4] H. Ansari et al. (2017) "Sequential Estimator: Toward efficient InSAR time series analysis".
[7] P.V.H. Vu et al. (2025) "Covariance Fitting Interferometric Phase Linking: Modular Framework and Optimization Algorithms".

Content

Conclusions

S-MLE-PL
Sequential Phase Linking based on Maximum Likelihood Estimation

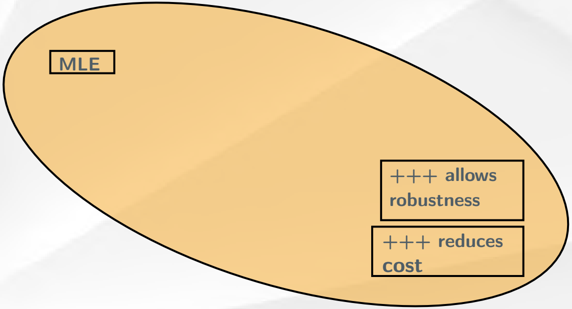

Conclusions

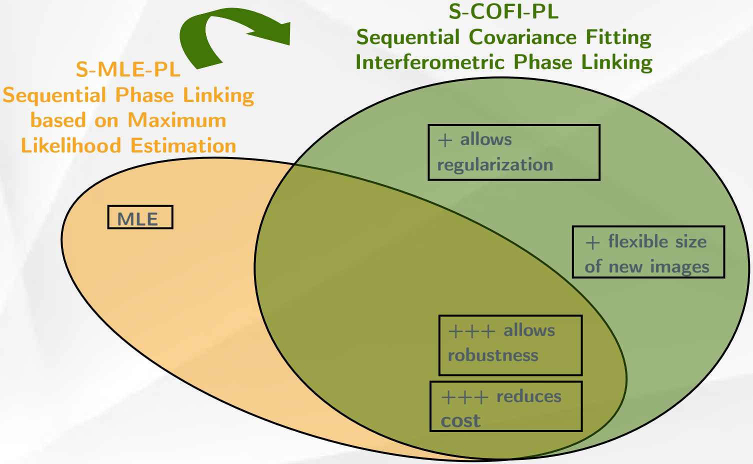

Conclusions

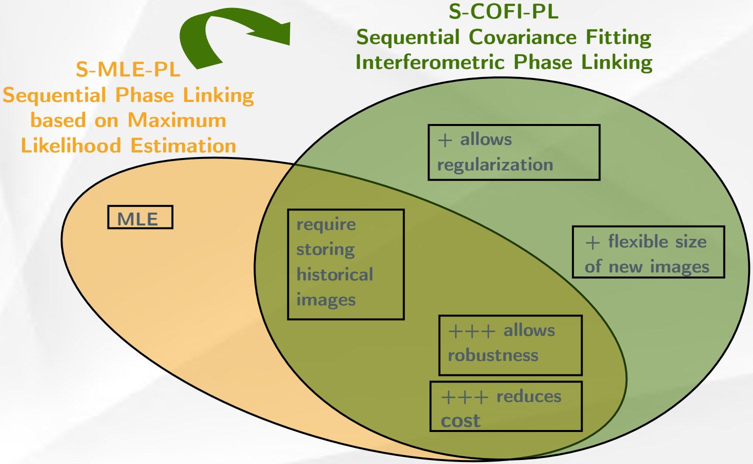

Conclusions

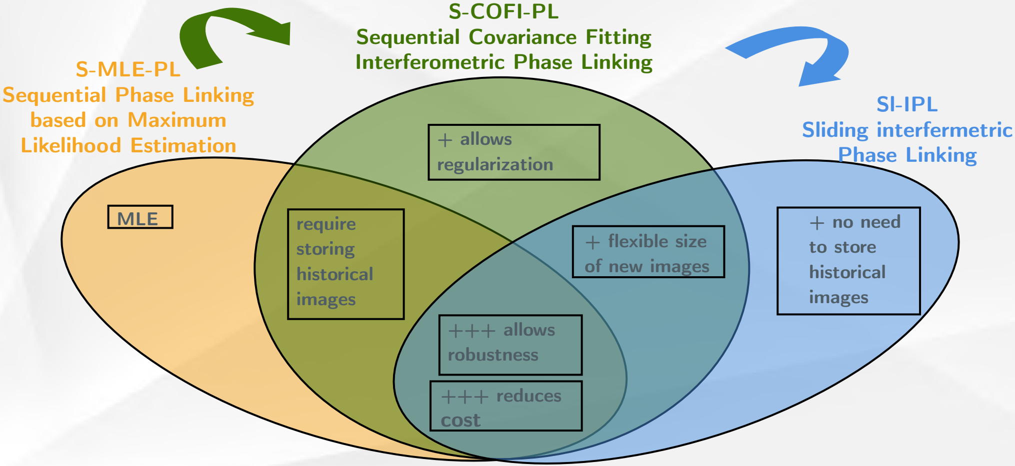

Perspectives (1/3)

Temporal monitoring of SAR image evolution (collab. with Mohammed Cherifi (Algeria))

Classic model:

$$x_{t_j}^i = \gamma_{t_j}^i e^{j\theta_{t_j}} + \epsilon_{t_j}^i$$

- ✗ no temporal dynamics
- ✗ prediction and/or interpolation is not possible

Perspectives (1/3)

Temporal monitoring of SAR image evolution (collab. with Mohammed Cherifi (Algeria))

Classic model:

$$x_{t_j}^i = \gamma_{t_j}^i e^{j\theta_{t_j}} + \epsilon_{t_j}^i$$

- ✗ no temporal dynamics
- ✗ prediction and/or interpolation is not possible

Proposed model:

$$x_{t_j}^i = \left(\qquad \right) e^{j \boxed{\theta_{t_j}}} + \epsilon_{t_j}^i$$

Auto-regressif mode (AR) model on the phase

$$\theta_{t_j} = \sum_{k=1}^{K} a_k \, \theta_{t_{j-k}} + b_j$$

Perspectives (1/3)

Temporal monitoring of SAR image evolution (collab. with Mohammed Cherifi (Algeria))

Classic model:

$$x^i_{t_j} = \gamma^i_{t_j} e^{j\theta_{t_j}} + \epsilon^i_{t_j}$$

- ✗ no temporal dynamics
- ✗ prediction and/or interpolation is not possible

Proposed model:

$$x^i_{t_j} = \left(\overline{\gamma}_0 \; e^{-\overline{\alpha} \;\; t_j} \qquad \right) e^{\; j \boxed{\theta_{t_j}}} + \epsilon^i_{t_j}$$

Auto-regressif mode (AR) model on the phase

$$\theta_{t_j} = \sum_{k=1}^{K} a_k \, \theta_{t_{j-k}} + b_j$$

Perspectives (1/3)

Temporal monitoring of SAR image evolution (collab. with Mohammed Cherifi (Algeria))

Classic model:

$$x^i_{t_j} = \gamma^i_{t_j} e^{j\theta_{t_j}} + \epsilon^i_{t_j}$$

- ✗ no temporal dynamics
- ✗ prediction and/or interpolation is not possible

Proposed model:

$$x^i_{t_j} = \left(\overline{\gamma}_0 \, e^{-\overline{\alpha} \; t_j} + \tilde{\gamma}_i \right) e^{\, j \boxed{\theta_{t_j}}} + \epsilon^i_{t_j}$$

Auto-regressif mode (AR) model on the phase

$$\theta_{t_j} = \sum_{k=1}^{K} a_k \, \theta_{t_{j-k}} + b_j$$

Perspectives (1/3)

Temporal monitoring of SAR image evolution (collab. with Mohammed Cherifi (Algeria))

Classic model:

$$x_{t_j}^i = \gamma_{t_j}^i e^{j\theta_{t_j}} + \epsilon_{t_j}^i$$

- ✗ no temporal dynamics
- ✗ prediction and/or interpolation is not possible

Proposed model:

$$x_{t_j}^i = \left(\boxed{\overline{\gamma}_0 \, e^{-\overline{\alpha} \, t_j} + \tilde{\gamma}_i} \right) e^{\, j \boxed{\theta_{t_j}}} + \epsilon_{t_j}^i$$

Mixed effects model on the coherence describing the temporal evolution

Auto-regressif mode (AR) model on the phase

$$\theta_{t_j} = \sum_{k=1}^{K} a_k \, \theta_{t_{j-k}} + b_j$$

Perspectives (1/3)

Temporal monitoring of SAR image evolution (collab. with Mohammed Cherifi (Algeria))

Classic model:

$$x^i_{t_j} = \gamma^i_{t_j} e^{j\theta_{t_j}} + \epsilon^i_{t_j}$$

- ✗ no temporal dynamics
- ✗ prediction and/or interpolation is not possible

Proposed model:

$$x^i_{t_j} = \left(\boxed{\overline{\gamma}_0 \; e^{-\overline{\alpha} \; t_j} + \tilde{\gamma}_i} \right) e^{\; j \boxed{\theta_{t_j}}} + \epsilon^i_{t_j}$$

Mixed effects model on the coherence describing the temporal evolution

Auto-regressif mode (AR) model on the phase

$$\theta_{t_j} = \sum_{k=1}^{K} a_k \; \theta_{t_{j-k}} + b_j$$

- ✓ temporal dynamics
- ✓ prediction and/or interpolation is possible

Perspectives (2/3)

$$\boxed{x_{t_j}^i = \left(\overline{\gamma}_0 \; e^{-\overline{\alpha} \; t_j} + \widetilde{\gamma}_i \right) \; e^{j \; (\sum_{k=1}^{K} a_k \theta_{t_{j-k}} + b_j)} + \epsilon_{t_j}^i}$$

- Latent vector: $z = (\widetilde{\gamma}_1, \ldots, \widetilde{\gamma}_n, \theta_1, \ldots, \theta_p)$
- Parameters: $\Theta = \{\overline{\gamma}_0, \overline{\alpha}, a_1, \ldots, a_K, \sigma_\gamma^2, \sigma_b^2, \sigma_\epsilon^2\}$

Perspectives (2/3)

$$x^i_{t_j} = \left(\overline{\gamma}_0 \ e^{-\overline{\alpha} \ t_j} + \widetilde{\gamma}_i \right) \ e^{j \ (\sum_{k=1}^{K} a_k \theta_{t_{j-k}} + b_j)} + \epsilon^i_{t_j}$$

- Latent vector: $z = (\widetilde{\gamma}_1, \ldots, \widetilde{\gamma}_n, \theta_1, \ldots, \theta_p)$
- Parameters: $\Theta = \{\overline{\gamma}_0, \overline{\alpha}, a_1, \ldots, a_K, \sigma^2_\gamma, \sigma^2_b, \sigma^2_\epsilon\}$
- **Stochastic Approximation Expectation Maximization (SAEM) algorithm**
  - **S-Step (Simulation):**

$$z_{(k)} \sim p(z \mid x, \Theta_{(k-1)})$$

  - **SA-Step (Stochastic Approximation):**

$$Q_{(k)}(\Theta) = Q_{(k-1)}(\Theta) + \gamma_{(k)} \left(\log p(x, z_{(k)} \mid \Theta) - Q_{(k-1)}(\Theta) \right)$$

  where $\gamma_{(k)}$ is a decreasing step-size sequence satisfying $\sum_k \gamma_{(k)} = +\infty$ and $\sum_k \gamma^2_{(k)} < +\infty$.
  - **M-Step (Maximization):**

$$\Theta_{(k)} = \arg\max_{\Theta} Q_{(k)}(\Theta)$$

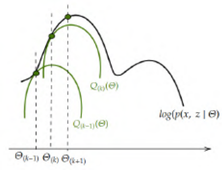

Perspectives (3/3)

First test on synthetic data

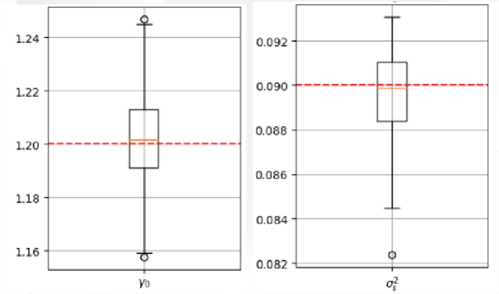

Figure: Boxplots of the estimated model parameters over 1000 Monte Carlo runs. The dashed red line indicates the true parameter value used to generate the synthetic data.

Perspectives (3/3)

First test on synthetic data

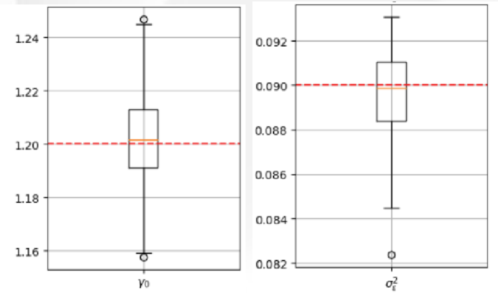

Figure: Boxplots of the estimated model parameters over 1000 Monte Carlo runs. The dashed red line indicates the true parameter value used to generate the synthetic data.

First test on real data: Mexico City

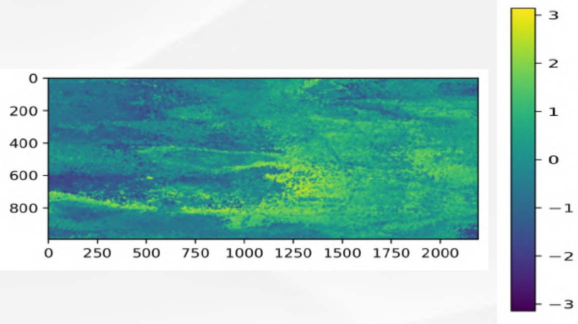

Figure: **Prediction of the phase difference at date 10 using the SAEM approach.**

⟶ **promising results**

Thank you for your attention !!

Journal Articles

[J1] **D. El Hajjar**, G. Ginolhac, Y. Yan and M. N. El Korso, "Robust Sequential Phase Estimation Using Multi-Temporal SAR Image Series," in IEEE Signal Processing Letters, vol. 32, pp. 811-815, 2025, doi: 10.1109/LSP.2025.3537334.

[J2] **D. El Hajjar**, G. Ginolhac, Y. Yan and M. N. El Korso, "Sequential Covariance Fitting for InSAR Phase Linking," in IEEE Transactions on Geoscience and Remote Sensing, vol. 63, pp. 1-13, 2025, Art no. 5215113, doi: 10.1109/TGRS.2025.3583566.

Conference Papers

[C1] **D. El Hajjar**, Y. Yan, G. Ginolhac and M. N. El Korso, "Sequential Phase Linking : Progressive Integration of SAR Images for Operational Phase Estimation," IGARSS 2024 - 2024 IEEE International Geoscience and Remote Sensing Symposium, Athens, Greece, 2024, pp. 11470-11473, doi: 10.1109/IGARSS53475.2024.10641742.

[C2] **D. El Hajjar**, A. Breloy, G. Ginolhac, M. N. El Korso and Y. Yan, "Sliding IPL: An efficient approach for estimating the phases of large SAR image time series" EUSIPCO 2025 - 2025 European Signal Processing Conference, Palermo, Italy, 2025, pp.

[C3] **D. El Hajjar**, G. Ginolhac, Y. Yan and M. N. El Korso, "Nouvelle approche pour l'estimation séquentielle et robuste de phase à partir de séries d'images SAR multi-temporelles". GRETSI, XXXème Colloque Francophone de Traitement du Signal et des Images, GRETSI, Aug 2025, Strasbourg, France.